

# Equivalent stress block for normal-strength concrete incorporating strain gradient effect

## Jun Peng

PhD Student, Department of Civil Engineering, The University of Hong Kong, Hong Kong

## Johnny Ching Ming Ho

Assistant Professor, Department of Civil Engineering, The University of Hong Kong, Hong Kong

## Hoat Joen Pam

Associate Professor, Department of Civil Engineering, The University of Hong Kong, Hong Kong

## Yuk Lung Wong

Associate Professor, Department of Civil and Structural Engineering, The Hong Kong Polytechnic University, Hong Kong

To account for the different behaviours of concrete under uniaxial compression and bending in the flexural strength design of reinforced concrete (RC) members, the stress–strain curve of concrete is normally scaled down so that the adopted maximum concrete stress in flexural members is less than the uniaxial strength. However, it was found from previous experimental research that the use of a smaller maximum concrete stress would underestimate the flexural strength of RC beams and columns. To investigate the effect of strain gradient on the maximum concrete stress developed in flexure, a total of 12 plain concrete and RC inverted T-shaped specimens were fabricated and tested under concentric and eccentric loads separately. The maximum concrete stress developed in the eccentric specimens was determined by modifying the concrete stress–strain curve obtained from the counterpart concentric specimens based on axial force and moment equilibriums. The test results revealed that the maximum concrete stress increases with strain gradient up to a certain maximum value. A formula was developed to correlate the maximum concrete stress to strain gradient. A pair of equivalent rectangular concrete stress block parameters that incorporate the effects of strain gradient was proposed for flexural strength design of RC members.

## Notation

$A_c$	area of concrete compression zone	$k_1$	ratio of average stress ( $f_{av}$ ) over compression area to maximum stress developed under flexure ( $f_{max}$ )
$A_g$	area of column cross-section	$k_2$	ratio of distance between extreme compressive fibre and resultant force of compressive stress block ( $P_c$ ) to that between the same fibre to neutral axis ( $c$ )
$A_s$	area of steel bar	$k_3$	ratio of $f_{max}$ to uniaxial concrete strength $f'_c$ or $f_{cu}$
$b$	width of cross-section	$M$	moment or flexural strength
$c$	neutral axis depth	$M_{ACI}$	moment calculated based on AIC 318M-08 (ACI, 2008)
$d$	distance of longitudinal steel bar to extreme compressive fibre (Equations 5, 6 and 7) or effective depth of cross-section	$M_{EC}$	moment calculated based on Eurocode 2 (CEN, 2004)
$E_s$	Young's modulus of steel bar	$M_{NZ}$	moment calculated based on NZS 3101 (SNZ, 2006)
$f_{av}$	average concrete compressive stress over compression area in flexural members	$M_p$	moment calculated based on the proposed values of equivalent rectangular concrete stress block parameters obtained in this study
$f'_c$	uniaxial concrete compressive strength represented by cylinder strength	$M_t$	measured moment capacity
$f_{cu}$	uniaxial concrete compressive strength represented by cube strength	$n$	number of longitudinal steel bars
$f_{max}$	maximum concrete compressive stress developed under flexure	$P$	axial load
$f_s$	stress of steel bar	$P_c$	resultant force of concrete compressive stress block
$f_y$	yield strength of steel bar	$x$	neutral axis depth
$h$	height of cross-section	$\alpha$	ratio of equivalent concrete compressive stress developed under flexure to concrete cylinder ( $f'_c$ ) or cube ( $f_{cu}$ ) strength

$\beta$	ratio between height of equivalent rectangular concrete compressive stress block and neutral axis depth
$\varepsilon$	concrete strain
$\varepsilon_{cu}$	ultimate concrete strain at extreme compressive fibre measured at maximum load of eccentrically loaded specimen
$\rho_s$	longitudinal reinforcement ratio
$\sigma$	concrete stress
$\sigma_c$	concrete compressive stress in concentrically loaded specimen
$\phi$	strain gradient

### Introduction

In flexural strength design of reinforced concrete (RC) members, it is essential to determine the concrete stress distribution in the compression zone when the extreme concrete fibre reaches a defined ultimate concrete strain. By assuming plane sections remain plane before and after bending, the strain distribution across the depth of section will be linear, as shown in Figure 1(b). The concrete stress distribution in the compression zone, which is obtained from its uniaxial stress–strain curve, is shown in Figures 1(c) and 1(d). These figures show that the actual concrete stress distribution is non-linear, which is defined by three parameters,  $k_1$ ,  $k_2$  and  $k_3$  (Attard and Stewart, 1998; Bae and Bayrak, 2003; Hognestad *et al.*, 1955; Ibrahim and MacGregor, 1996, 1997; Kaar *et al.*, 1978; Ozbakkaloglu and Saatcioglu, 2004; Sheikh and Uzumeri, 1980; Soliman and Yu, 1967; Tan and Nguyen, 2004, 2005).  $k_1$  is the ratio of average stress  $f_{av}$  over the compression area to maximum stress developed under flexure  $f_{max}$ ;  $k_2$  is the ratio of distance between the extreme compressive fibre and the resultant force of the stress block ( $P_c$ ) to that between the same fibre to the neutral axis ( $c$ );  $k_3$  is the ratio of  $f_{max}$  to uniaxial concrete strength  $f'_c$  or  $f_{cu}$ .

Since the actual concrete stress distribution is non-linear, it is relatively cumbersome to use it directly in the practical flexural strength design of RC members. Therefore, in practice, the actual concrete stress block is replaced by an equivalent rectangular concrete stress block as shown in Figure 1(e), which has the same

area and centroid as the actual concrete stress distribution under flexure. In this case,  $k_1$ ,  $k_2$  and  $k_3$  are combined and expressed in terms of  $\alpha$  and  $\beta$ , which are the parameters of the equivalent rectangular concrete stress block commonly adopted in various current RC design codes (ACI, 2008; CEN, 2004; SNZ, 2006):

$$1. \quad k_1 k_3 = \alpha \beta$$

$$2. \quad k_2 = 0.5 \beta$$

where  $\alpha$  is the ratio of equivalent concrete compressive stress developed under flexure to concrete cylinder ( $f'_c$ ) or cube ( $f_{cu}$ ) strength and  $\beta$  is the ratio of the height of equivalent rectangular concrete compressive stress block to neutral axis depth ( $c$ ). An ideal equivalent rectangular concrete stress block should give a precise representation of the magnitude and location of the resultant concrete compressive force in order to provide an accurate estimate of the flexural strength of RC members.

The currently adopted values of  $\alpha$  and  $\beta$  in the aforementioned RC design codes for the flexural strength design of RC members are summarised in Table 1, which shows that the values of  $\alpha$  and  $\beta$  are dependent only on the concrete strength. To study the accuracy of  $\alpha$  and  $\beta$  values for flexural strength estimation, a comparison of the theoretical strengths of RC members predicted by the American Concrete Institute code AIC 318M-08 (ACI, 2008) ( $M_{ACI}$ ), Eurocode 2 (CEN, 2004) ( $M_{EC}$ ) and the New Zealand code NZS 3101 (SNZ, 2006) ( $M_{NZ}$ ) with their corresponding measured flexural strengths  $M_t$  tested by some researchers (Debernardi and Taliano, 2002; Lam *et al.*, 2003; Mo and Wang, 2000; Pecce and Fabbrocino, 1999) is summarised in Table 2: the theoretical strengths are consistently smaller than the measured strengths and the maximum underestimation in flexural strength can reach 23%. This indicates that the values for  $\alpha$  and  $\beta$  stipulated in the current RC design codes are underestimated. It should be noted that the underestimation of flexural strength of

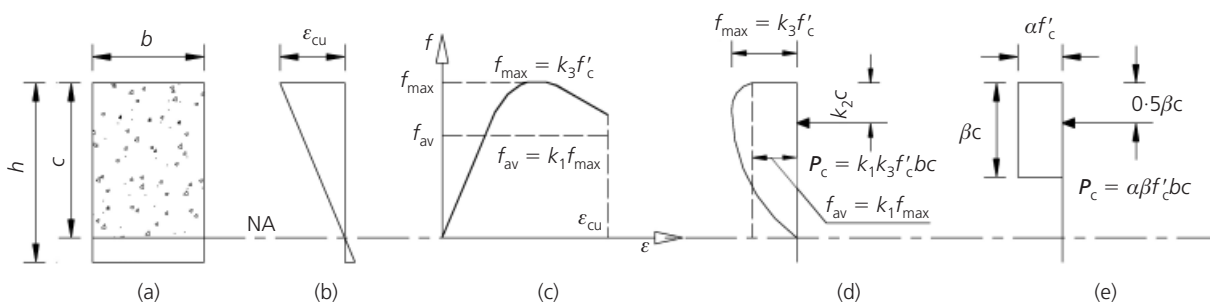


Figure 1. Concrete stress block parameters: (a) cross-section; (b) strain distribution; (c) stress–strain curve under flexure; actual stress distribution at ultimate state; (d) actual stress distribution at ultimate state; (e) equivalent rectangular stress block

Design code	$\alpha$		$\beta$	
ACI 318M-08 (ACI, 2008)	0.85	for all $f'_c$	0.85	for $f'_c \leq 28$ MPa
Eurocode 2 (CEN, 2004)*	0.85	for $f'_c \leq 50$ MPa	0.85–0.007( $f'_c - 28$ ) $\geq$ 0.65	for $f'_c > 28$ MPa
NZS 3101 (SNZ, 2006)	0.85–0.85[( $f'_c - 50$ )/200]	for $50 < f'_c \leq 90$ MPa	0.8–[( $f'_c - 50$ )/400]	for $f'_c \leq 50$ MPa
	0.85	for $0 < f'_c \leq 55$ MPa	0.85	for $0 < f'_c \leq 30$ MPa
	0.85–0.004( $f'_c - 55$ )	for $55 < f'_c \leq 80$ MPa	0.85–0.008( $f'_c - 30$ )	for $30 < f'_c \leq 55$ MPa
	0.75	for $f'_c > 80$ MPa	0.65	for $f'_c > 55$ MPa

\* Based on UK National Annex

**Table 1.** Values of  $\alpha$  and  $\beta$  stipulated in various current RC design codes

Specimen code	$f'_c$ : MPa	$M_{ACI}$ : kNm (1)	$M_{EC}$ : kNm (2)	$M_{NZ}$ : kNm (3)	$M_t$ : kNm (4)	(1) (4)	(2) (4)	(3) (4)
Beams								
A*	41.3	97.0	97.0	97.0	104.0	0.93	0.93	0.93
B*	41.3	45.0	45.0	45.0	49.6	0.91	0.91	0.91
T3†	27.7	28.9	29.3	28.9	32.5	0.89	0.90	0.89
T6†	27.7	171.0	171.0	171.0	192.0	0.89	0.89	0.89
Columns								
C1–2‡	26.7	304.0	308.0	304.0	375.0	0.81	0.82	0.81
C2–2‡	27.1	325.0	331.0	325.0	400.0	0.81	0.83	0.81
X6§	31.9	28.5	29.0	28.6	37.1	0.77	0.78	0.77
X7§	35.7	29.7	30.5	29.8	37.1	0.80	0.82	0.80

\* Pecce and Fabbrocino (1999)

† Debernardi and Taliano (2002)

‡ Mo and Wang (2000)

§ Lam *et al.* (2003)

**Table 2.** Comparison of flexural strengths obtained from codes and previous tests

beams and columns should be treated with caution because it will underestimate the shear demand of the members (Pam and Ho, 2001). Failure due to shear would be very brittle and should be avoided in design (Baczowski and Kuang, 2008; Bukhari *et al.*, 2010; Choi *et al.*, 2010; Lu *et al.*, 2009). A precise estimation of the beams' flexural strength would also allow engineers to predict the locations of plastic hinges (Bai and Au, 2008; Jaafar, 2008; Pam and Ho, 2009) and hence the deformability (Ho and Pam, 2010; Sebastian and Zhang, 2008; Wu *et al.*, 2004) of members under extreme events. Engineers may then correctly design and detail the reinforcement within the plastic hinge region for the required ductility and rotation capacity (Spence, 2008; Zhou and Zheng, 2010).

In fact, the maximum concrete compressive stress that can be developed in the presence of a strain gradient (i.e. the ratio of

extreme compressive concrete fibre strain to neutral axis depth) could be studied by the factor  $k_3$ , and the equivalent concrete stress by  $\alpha$ . In the past, much experimental research has been conducted to investigate the range of  $k_3$  for RC members (Hognestad *et al.*, 1955; Kaar *et al.*, 1978; Sheikh and Uzumeri, 1980; Soliman and Yu, 1967). The test results in this study revealed the following.

- (a) The range of  $k_3$  varied mostly from 0.8 to 1.0 for concentrically loaded columns and from 0.9 to 1.0 for eccentrically loaded columns;  $\alpha$  varied from 0.8 to 1.0 for both columns. These results indicate that the maximum concrete stress that can be developed in concrete under flexure could be larger than that stipulated in the current RC design codes.
- (b) The test results on  $k_3$  and  $\alpha$  are fairly scattered. This implies

that the values of  $k_3$  and  $\alpha$  depend on other factors apart from just the uniaxial concrete cylinder/cube strength.

In this work, the effect of strain gradient on the maximum concrete compressive stress that can be developed under flexure as compared with its uniaxial strength was experimentally investigated. A total of 12 (divided into five groups) plain concrete (PC) and RC column specimens with concrete strength 22–49 MPa were fabricated and tested. The cross-section properties of the specimens in each group were identical, and one specimen in each group was subjected to concentric loading while the rest were subjected to eccentric loading. From the results, ratios of the maximum concrete compressive stress ( $f_{max}$ ) developed in the eccentrically loaded specimens to the maximum uniaxial compressive stress ( $\sigma_c$ ) developed in the concentrically loaded specimens were determined. The equivalent concrete stress block parameters  $\alpha$  and  $\beta$  for the tested specimens were also derived based on the obtained ratios. It was found that the values of  $\alpha$  were dependent on strain gradient apart from concrete strength, while those of  $\beta$  remained relatively constant with strain gradient and concrete strength. Formulas incorporating the effects of strain gradient were developed for the equivalent rectangular concrete stress block parameters  $\alpha$  and  $\beta$ .

## Experimental programme

### Details of test specimens

In total, 12 (groups 1 to 5) inverted T-shaped specimens were fabricated and tested in this study. Group 1 consisted of a pair of PC specimens, each of groups 2 to 4 consisted of a pair of RC specimens and group 5 consisted of four RC specimens. One of the specimens in each group was tested with concentric load while the rest were tested with eccentric load. All the specimens in each group had identical cross-sections and materials properties. The cross-section dimensions of columns and beams in all the specimens were identical ( $400 \times 400 \text{ mm}^2$ ). The column height was 1400 mm and the length of the beam was 1500 mm. Figure 2 shows the steel reinforcement details of the specimens. The test area of the specimens was in the middle 800 mm length of the column; the rest of the specimen was much more heavily reinforced. The PC specimens did not contain any longitudinal reinforcement steel within the test area, while the RC specimens contained different amounts of longitudinal steel ratios (from 0.42 to 1.18%). The cross-sections of the test specimens were those commonly adopted by other researchers (Choi *et al.*, 2009; Han *et al.*, 2010; Sim *et al.*, 2009). Table 3 summarises the section properties of all the specimens. In the specimen codes, the first number refers to the concrete strength on day 28 and the second number refers to the longitudinal steel ratio.

In each group of specimens, one was tested under concentric compressive axial load to obtain the uniaxial behaviour of concrete, while the counterpart specimen(s) was/were tested under eccentric load with different eccentricities to simulate different extents of strain gradient. The eccentricities applied to

these columns were varied from 100 to 140 mm for different columns, as summarised in Table 3. The applied eccentricity has a direct implication on the specimen's failure mode. When the column is subjected to small eccentricity, it would fail in compression where the tension steel would not yield. However, when the column is subjected to large eccentricity, it would fail in tension where the tension steel would yield. The two failure modes are located in two different regions on the column interaction curve as shown in Figure 3.

The column specimen subjected to concentric load in each group was not subjected to strain gradient and served as the reference specimen; the counterpart specimens were all subjected to strain gradient. The axial load applied to the column was produced by a computerised electro-hydraulic servo-controlled multi-purpose testing machine having a maximum compressive loading capacity of 10 000 kN. Figure 4 shows the test setup of the specimens subjected to concentric and eccentric loading.

### Instrumentation

Strain gauges for both steel and concrete were used. Steel strain gauges were attached to longitudinal steel bars located within the testing region to measure axial and bending strains and a concrete strain gauge was attached on each face of every concentric specimen. For the eccentrically loaded specimens, 12 strain gauges (two on each bending face and four on each face perpendicular to the bending face) were attached to every specimen to measure the concrete strain distribution within the elastic range. Details of the strain gauges are shown in Figure 5.

For each specimen, 12 linear variable differential transducers (LVDTs) were installed on four sides of the specimen within the test area to measure the deformation due to axial load and/or bending moment. Two LVDTs were installed on each of the bending faces and four LVDTs were installed on each side perpendicular to the bending face. Details of the LVDTs are also shown in Figure 5.

### Test procedure

For the specimens subjected to concentric load, a 20 mm steel plate was installed on top of the column to ensure a smooth contact during loading application. On the contrary, for specimens subjected to eccentric load, a guided steel roller was installed at a prescribed eccentricity on top of the steel plate. Apart from providing a smooth contact surface, this steel plate also increased the bearing capacity of the column to avoid premature local failure. Loading was applied to all the specimens in a displacement-controlled manner at a rate of 0.36 mm/min. All the data were recorded on a datalogger. Loading was terminated when it had reached more than 80% of the maximum value.

## Test results and discussion

### Test observations

In all the specimens, the applied axial load initially increased linearly as the axial displacement of the column increased prior

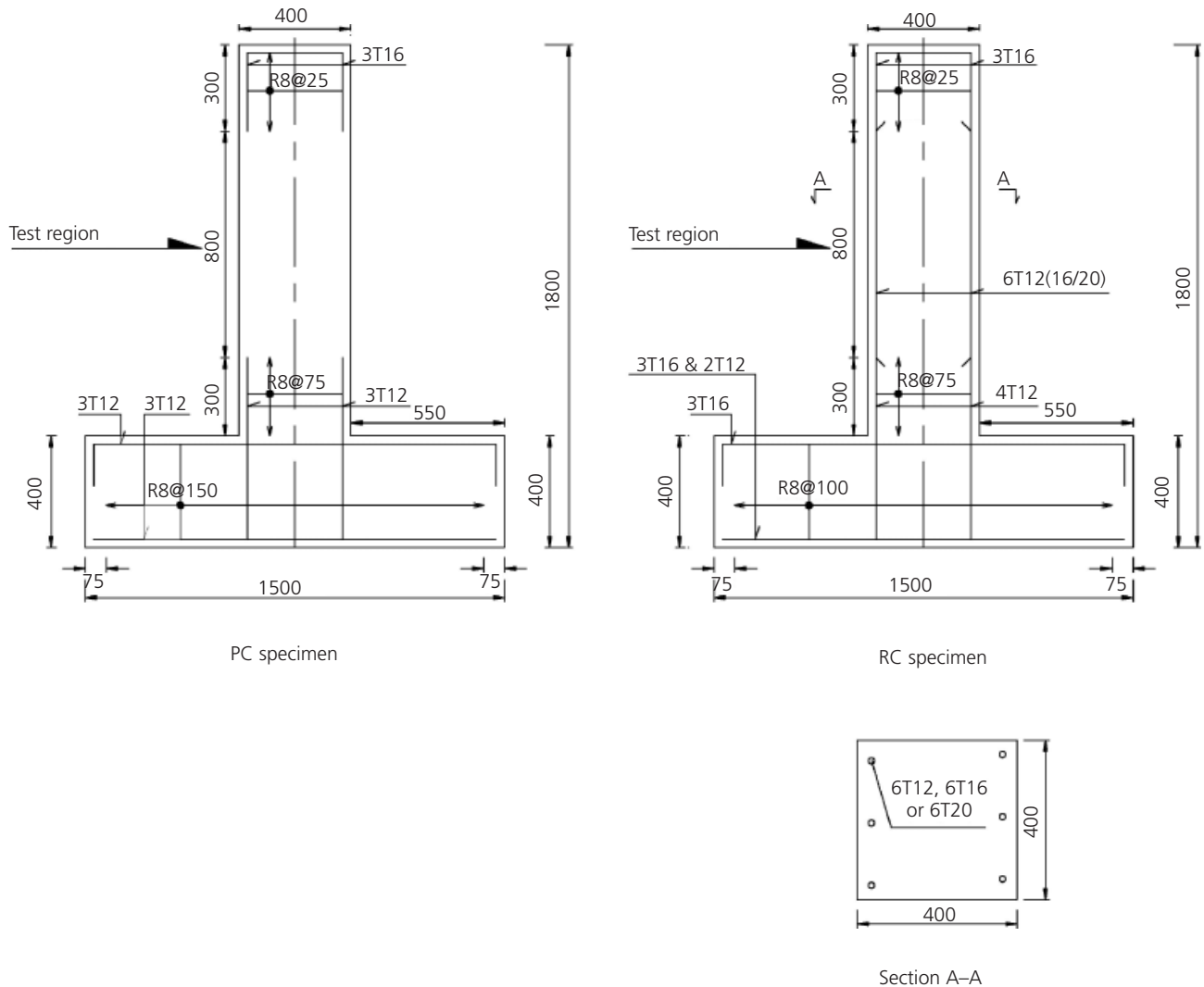


**Figure 2.** Details of steel reinforcement. All dimensions in millimetres; concrete cover 20 mm

to reaching about 50% of the maximum axial load. At this stage, no significant damage was observed in the concentrically loaded specimens, and flexural cracks or concrete crushing were not observed in the eccentrically loaded specimens. Subsequently, the axial displacement of the columns increased more rapidly as the stiffness reduced. When the applied load reached the maximum value, concrete cracking or crushing and cover spalling were observed.

In all the concentrically loaded specimens, compression crushes occurred around the mid-height of the columns, accompanied by inelastic buckling of the longitudinal steel. For the eccentrically loaded PC specimens, concrete crushing on the compression side and flexural cracking on the tension side were observed, accompanied by a large rotation of the column top. For the eccentrically loaded RC specimens, inelastic buckling of longitudinal steel and a diagonal concrete crack crossing the test area were observed in

addition to concrete crushing and flexural cracks. Figure 6 shows the conditions of two selected groups of specimens after failure.

#### Test results of concentrically loaded specimens

The measured concrete compressive force of the concentrically loaded column specimens is plotted against the axial displacement of the column in Figure 7 on the primary axis. For the PC specimens, the total concrete compressive force is equal to the compressive axial load applied by the hydraulic servo-actuator. However, for the RC specimens, the total concrete compressive force was obtained by subtracting the compressive force contributed by the longitudinal steel from the applied axial load.

Figure 7 shows concrete compressive stress plotted against concrete strain for the concentrically loaded specimens. The concrete stress was evaluated based on the gross area of concrete with steel area being subtracted in the RC specimens. The

Specimen code	Loading	Longitudinal steel				$f'_c$ : MPa		Eccentricity: mm
		$\rho_s$ : %	Detail	$f_y$ : MPa	$E_s$ : GPa	28th day	Testing day	
Group 1								
PC30-0-CON	Concentric	0	—	—	—	29.6	30.0	0
PC30-0-ECC	Eccentric	0	—	—	—	29.6	29.3	120
Group 2								
RC22-0.42-CON	Concentric	1.42	6T12	538	203	22.2	28.7	0
RC22-0.42-ECC	Eccentric	0.42	6T12	538	203	22.2	28.7	140
Group 3								
RC22-0.75-CON	Concentric	0.75	6T16	533	203	21.9	27.4	0
RC22-0.75-ECC	Eccentric	0.75	6T16	533	203	21.9	26.8	140
Group 4								
RC31-1.18-CON	Concentric	1.18	6T20	536	200	30.7	34.5	0
RC31-1.18-ECC	Eccentric	1.18	6T20	536	200	30.7	34.3	110
Group 5								
RC46-0.75-CON	Concentric	0.75	6T16	515	203	45.6	45.6	0
RC46-0.75-ECC-1	Eccentric	0.75	6T16	515	203	45.6	46.6	100
RC46-0.75-ECC-2	Eccentric	0.75	6T16	515	203	45.6	48.6	120
RC46-0.75-ECC-3	Eccentric	0.75	6T16	515	203	45.6	48.6	140

Table 3. Section properties and applied eccentricities

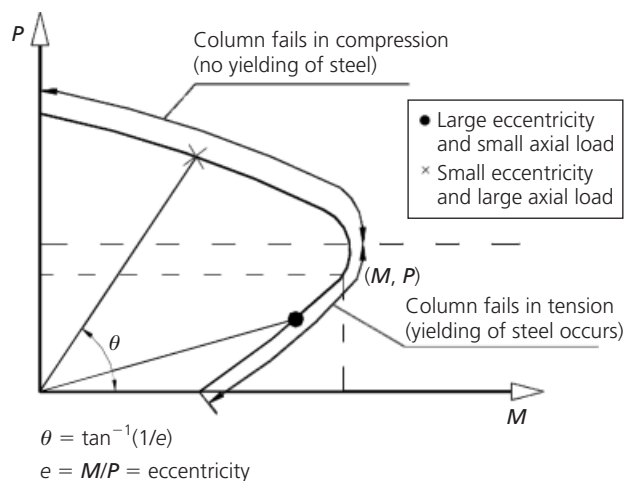


Figure 3. Failure modes and column interaction diagram

concrete strain was taken as the average reading of all the LVDTs installed on all the column faces divided by the gauge length. These concrete stress–strain curves are used later in the paper to evaluate the maximum concrete compressive stress that can be developed in the counterpart eccentrically loaded specimens.

From Figure 7 it is evident that:

- (a) the concrete compressive force–displacement and concrete compressive stress–strain curves are fairly linear up to about 50% of the maximum force (stress), after which the

displacement (strain) increases more rapidly than the concrete compressive force (stress)

- (b) the measured maximum concrete stress is very close to its uniaxial cylinder concrete strength

- (c) specimens with higher concrete strength have a larger initial elastic stiffness.

### Test results of eccentrically loaded specimens

The measured concrete compressive force of the eccentrically loaded specimens is plotted against axial displacement of the column in Figure 8. The concrete compressive forces of the RC specimens were obtained by subtracting the steel force from the total load. The maximum moments acting on the specimens were evaluated by multiplying the obtained axial load by the eccentricity. These axial loads and moments are used later in the paper to back-calculate concrete stress distribution within the compression zone of the eccentrically loaded specimens.

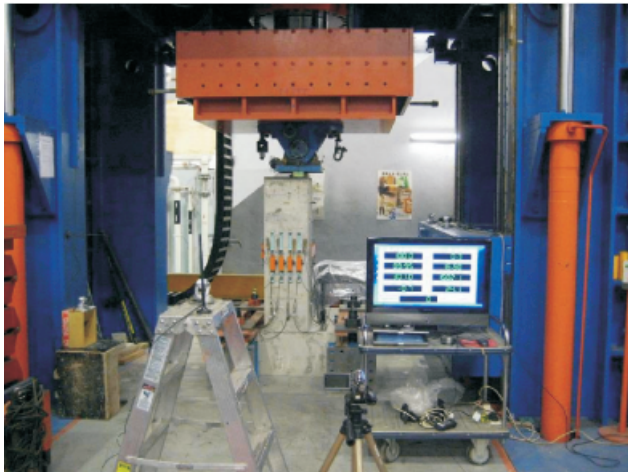
### Derivation of concrete stress block parameters

#### Derivation of $k_1$ , $k_2$ and $k_3$

The effect of strain gradient on the maximum compressive stress that can be developed in concrete was investigated by determining the ratio of maximum concrete compressive stress developed in the eccentrically loaded specimens ( $f_{max}$ ) to that in the concentrically loaded counterpart specimens ( $\sigma_c$ ), which is equal to  $k_3$ . The value of  $k_3$  can be evaluated by equating the theoretical with the measured axial force and moment of the eccentrically loaded specimens. The theoretical values were computed based



(a)



(b)

**Figure 4.** Test setup under: (a) concentric loading and (b) eccentric loading

on the stress–strain curve obtained from the concentrically loaded specimens multiplied by  $k_3$  to take into account the effects of strain gradient. A numerical analysis method was developed and adopted to determine the value of  $k_3$  for all the eccentrically loaded specimens.

At first, the stress–strain curve of each concentrically loaded specimen was obtained by fitting the measured stress and strain data using the parabolic function:

$$3. \quad \sigma = A\varepsilon^2 + B\varepsilon$$

where  $\sigma$  and  $\varepsilon$  are the concrete stress and strain developed in concentrically loaded specimens respectively, and  $A$  and  $B$  are coefficients obtained from regression analysis.

From the definition of  $k_3$ , the concrete stress–strain curve devel-

oped in eccentrically loaded specimens under strain gradient can be obtained by multiplying both sides of Equation 3 by  $k_3$ :

$$4. \quad k_3\sigma = k_3(A\varepsilon^2 + B\varepsilon)$$

The next step is to determine numerically the value of  $k_3$  for the eccentrically loaded specimens to assess the effects of strain gradient on the stress–strain curve of concrete. The value of  $k_3$  for each eccentrically loaded specimen can be determined by considering the axial force ( $P$ ) and moment ( $M$ ) equilibriums of the column section, which are expressed in Equations 5a and 5b respectively (compression is taken as positive):

$$5a. \quad P = \int_{A_c} k_3 (A\varepsilon^2 + B\varepsilon) dA_c + \sum_{i=1}^n f_{si}A_{si}$$

$$5b. \quad M = \int_{A_c} k_3 (A\varepsilon^2 + B\varepsilon) \left( \frac{h}{2} - c + x \right) dA_c + \sum_{i=1}^n f_{si}A_{si} \left( \frac{h}{2} - d_i \right)$$

$$5c. \quad \varepsilon = \frac{x}{c} \varepsilon_{cu}$$

where  $A_c$  is the area of concrete compression zone,  $x$  is the distance of strip  $dA_c$  from the neutral axis,  $n$  is the total number of steel bars,  $f_{si}$  and  $A_{si}$  are respectively the stress and area of the  $i$ th steel bar,  $d_i$  is the distance of the  $i$ th steel bar from the extreme concrete compressive fibre and  $\varepsilon_{cu}$  is the ultimate concrete strain. The ultimate concrete strain is the concrete strain at extreme compressive fibre when the eccentrically loaded specimens reached the maximum moment (Park and Paulay, 1975).

In this study, the neutral axis depth  $c$  is treated as an unknown to be determined from the axial force and moment equilibrium equations (Equations 5). Although the neutral axis depth could be obtained approximately by linear interpolating the concrete strains obtained by LVDTs at the extreme compression and tension fibres, the value of such was not adopted in the evaluation of  $k_3$  because the concrete strain at extreme tension fibre is a very small and localised value. Hence, the measurement of average concrete tensile strain over the gauge length of LVDTs will underestimate the actual tensile strain of concrete and subsequently overestimate the neutral axis depth. Instead of using the neutral axis depth obtained from direct measurement, its computational value based on the axial force and moment equilibriums would be more reliable.

By substituting Equation 5c into Equations 5a and 5b,  $P$  by the

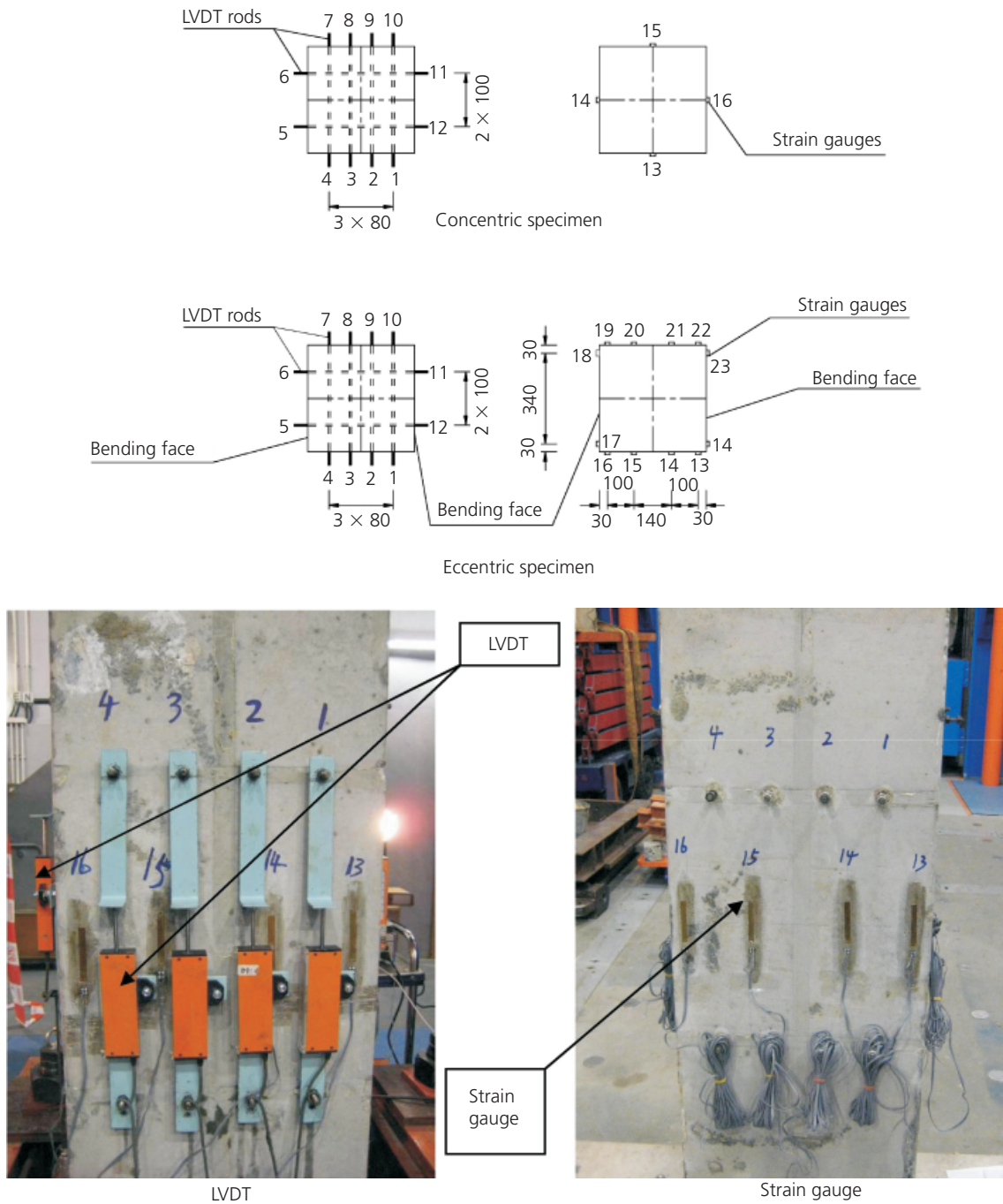


Figure 5. Details of instrumentation

measured axial load in Equation 5a and  $M$  by the measured moment in Equation 5b,  $k_3$  and  $c$  can be solved simultaneously. Accordingly,  $k_1$  and  $k_2$  can be solved respectively from Equations 6a and 6b:

$$6a. \quad P = k_1 k_3 \sigma_c b c + \sum_{i=1}^n f_{si} A_{si}$$

$$6b. \quad M = k_1 k_3 \sigma_c b c \left( \frac{h}{2} - k_2 c \right) + \sum_{i=1}^n f_{si} A_{si} \left( \frac{h}{2} - d_i \right)$$

where  $\sigma_c$  is the maximum concrete compressive stress measured in the concentrically loaded specimen.



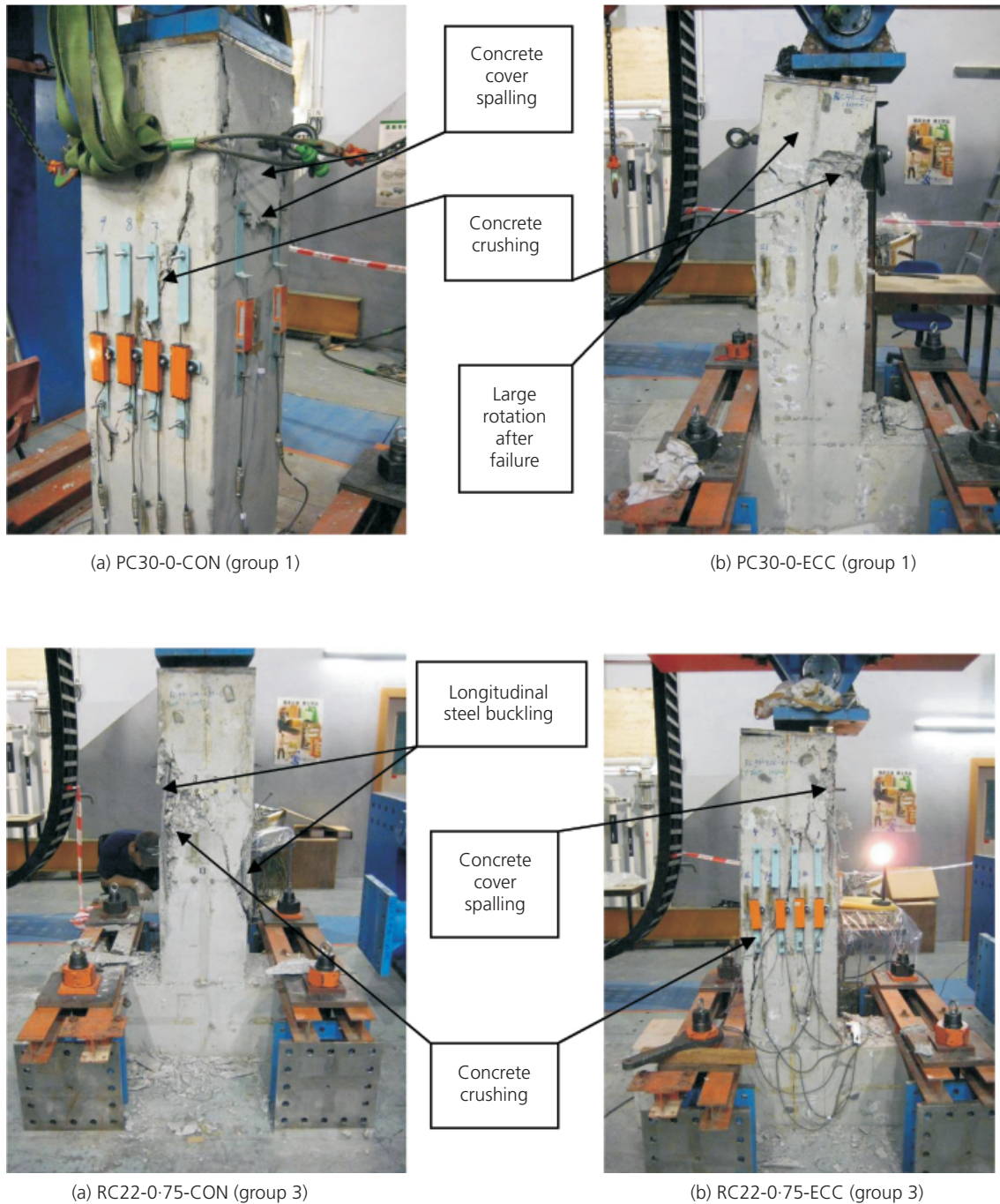


Figure 6. Observed behaviour of some test specimens

The values of  $k_1$ ,  $k_2$ ,  $k_3$  and  $c$  evaluated for the eccentrically loaded specimens are listed in Table 4 together with their corresponding  $\sigma_c$  and strain gradient  $\phi$  (in rad/m), which is equal to  $\varepsilon_{cu}/c$ . The table shows that the value of  $k_3$  increases as  $\phi$  increases. Therefore, it is evident that an increase in strain gradient would enhance the maximum concrete stress developed in RC members under flexure. However, the values of  $k_1$  and  $k_2$  remain relatively constant with the strain gradient.

The average values of  $k_1$ ,  $k_2$  and  $k_3$  are compared with the values obtained by other researchers (Hognestad *et al.*, 1955; Kaar *et al.*, 1978; Mansur *et al.*, 1997; Swartz *et al.*, 1985; Tan and Nguyen, 2004, 2005) in Table 5. The average value of  $k_2$  obtained in this study is mostly slightly smaller than that obtained by other researchers, but the average value of  $k_3$  obtained in this study is significantly larger. This indicates that the maximum compressive stress developed in concrete under flexure should be larger.

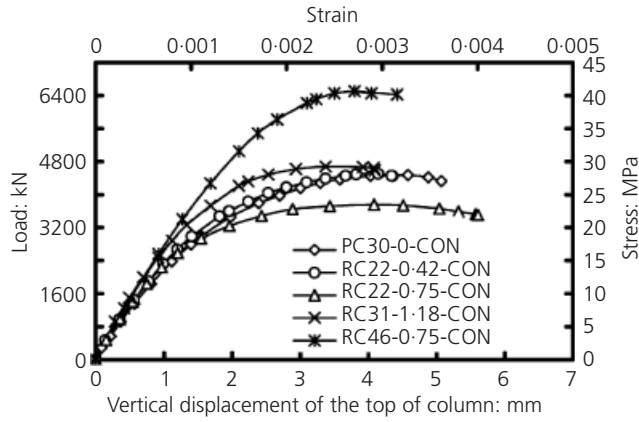


Figure 7. Load–displacement and stress–strain curves of concrete of concentrically loaded specimens

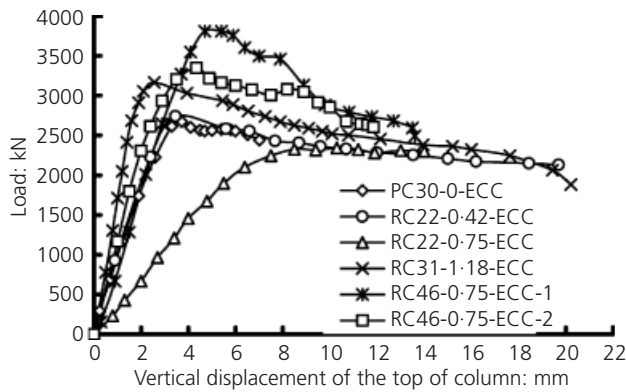


Figure 8. Load–displacement curves of concrete of eccentrically loaded specimens

Furthermore, it is also seen that the value of the product  $k_1k_3$  obtained in this study is generally larger than the values obtained by other researchers. This therefore reveals that the total compressive force that could be developed by concrete under flexure should also be larger. Further investigation into the internal mechanism within the concrete member that leads to a higher maximum compressive stress under strain gradient is required.

#### Derivation of equivalent rectangular concrete stress block parameters

To determine the effect of strain gradient on the equivalent rectangular concrete stress block parameters, the values of  $\alpha$  and  $\beta$  of the eccentrically loaded specimens are firstly evaluated and compared with the respective values of the concentrically loaded specimens. The value of  $\alpha$  for the concentrically loaded specimens can be determined from Equation 7a, while the values of  $\alpha$  and  $\beta$  for the eccentrically loaded specimens can be determined from Equations 7b and 7c, which were derived based on axial force and moment equilibrium conditions as shown in Figure 1(e).

$$7a. \quad P = \alpha f'_c b h$$

$$7b. \quad P = \alpha \beta f'_c b c + \sum_{i=1}^n f_{si} A_{si}$$

$$7c. \quad M = \alpha \beta f'_c b c \left( \frac{h}{2} - \frac{\beta}{2} c \right) + \sum_{i=1}^n f_{si} A_{si} \left( \frac{h}{2} - d_i \right)$$

Specimen code	$f'_c$ : MPa (testing day)	$\alpha_c$ : MPa	$c$ : mm	$k_1$	$k_2$	$k_3$	$k_1k_3$	$\epsilon_{cu}$	$\phi$ : rad/m	$d/c$
Plain concrete specimen										
PC30-0-ECC	29.3	28.1	199	0.683	0.401	1.68	1.14	0.0035	0.018	2.01*
Reinforced concrete specimens										
RC22-0-42-ECC	28.7	28.1	218	0.656	0.403	1.63	1.07	0.0031	0.014	1.72
RC22-0-75-ECC	26.8	23.5	229	0.691	0.392	1.54	1.06	0.0031	0.014	1.62
RC31-1-18-ECC	34.3	29.3	287	0.642	0.397	1.11	0.713	0.0029	0.010	1.29
RC46-0-75-ECC-1	46.6	40.1	297	0.581	0.383	1.05	0.610	0.0031	0.010	1.23
RC46-0-75-ECC-2	48.6	40.1	252	0.581	0.393	1.30	0.755	0.0035	0.014	1.44
RC46-0-75-ECC-3	48.6	40.1	223	0.558	0.383	1.35	0.754	0.0030	0.014	1.63
Average	37.6	32.8	—	0.627	0.393	1.38	0.872	0.0031	—	—

\*  $d$  is effective depth of RC specimens and is taken as the overall depth of column for the PC specimen

Table 4. Values of  $k_1$ ,  $k_2$  and  $k_3$

Research	$f'_c$ : MPa	$k_1$	$k_2$	$k_3$	$k_1 k_3$
Hognestad <i>et al.</i> (1955)	27.6	0.790	0.450	0.940	0.743
Hognestad <i>et al.</i> (1955)	34.5	0.750	0.440	0.920	0.690
Kaar <i>et al.</i> (1978)	45.0	0.722	0.400	0.970	0.700
Swartz <i>et al.</i> (1985)	57.0	0.714	0.415	0.980	0.700
Mansur <i>et al.</i> (1997)	57.2	0.704	0.420	0.980	0.690
Tan and Nguyen (2004, 2005)	48.3	0.700	0.380	0.930	0.651
This study	37.6	0.627	0.393	1.38	0.872

**Table 5.** Comparison of values of  $k_1$ ,  $k_2$  and  $k_3$

Specimen code	$\alpha$	$\beta$	$\varepsilon_{cu}$	$\phi$ : rad/m	$d/c$
PC30-0-CON	0.937	—	—	0.0	0.0*
RC22-0.42-CON	0.819	—	—	0.0	0.0
RC22-0.75-CON	0.858	—	—	0.0	0.0
RC31-1.18-CON	0.849	—	—	0.0	0.0
RC46-0.75-CON	0.840	—	—	0.0	0.0
Average	0.866	—	—	0.0	0.0
PC30-0-ECC	1.43	0.802	0.0035	0.018	2.01*
RC22-0.42-ECC	1.32	0.806	0.0031	0.014	1.72
RC22-0.75-ECC	1.36	0.783	0.0031	0.014	1.62
RC31-1.18-ECC	0.90	0.794	0.0029	0.010	1.29
RC46-0.75-ECC-1	0.80	0.765	0.0031	0.010	1.23
RC46-0.75-ECC-2	0.96	0.785	0.0035	0.014	1.44
RC46-0.75-ECC-3	0.99	0.765	0.0030	0.014	1.63
Average	1.11	0.786	0.0031	—	—

\*  $d$  is effective depth of RC specimens and is taken as the overall depth of column for the PC specimen

**Table 6.** Values of equivalent rectangular stress block parameters and strain gradient

The neutral axis depth  $c$  evaluated from Equation 5 is adopted in solving the above equations for  $\alpha$  and  $\beta$ , which are listed in Table 6, using the measured axial load  $P$  and moment  $M$ . The values of  $\alpha$  for the concentrically loaded specimens are also listed in Table 6. The following points can be concluded.

- The value of  $\alpha$  for the eccentrically loaded specimens subjected to strain gradient is larger than that of the respective concentrically loaded specimens. This therefore implies that strain gradient could enhance the equivalent concrete stress developed in flexural RC members
- The value of  $\alpha$  for the eccentrically loaded specimens increases as the strain gradient increases, but decreases as the concrete strength increases.
- The average value of  $\alpha$  obtained for the concentrically loaded columns (with  $f'_c = 30\text{--}46$  MPa) is about 0.866, which is very close to the current design value of  $\alpha = 0.85$  stipulated

in AIC 318M-08 (ACI, 2008), the UK National Annex to Eurocode 2 (CEN, 2004) and NZS 3101 (SNZ, 2006).

It can thus be concluded that the current design codes can predict the strengths of RC columns subjected to pure axial load without strain gradient fairly accurately, but would underestimate the strengths of RC beams and columns subjected to flexure with or without axial load where strain gradient exists.

#### Effects of strain gradient on stress block parameters

It can be easily observed from Tables 4 and 6 that the values of  $k_3$  and  $\alpha$  actually depend on the strain gradient rather than just the uniaxial concrete strength. Table 4 shows that  $k_3$  increases as the strain gradient increases, while  $k_1$  and  $k_2$  remain relatively constant with strain gradient. Similarly,  $\alpha$  increases with strain gradient, while  $\beta$  remains relatively constant (Table 6).

Variation of the stress block parameters with the strain gradient is now determined. However, since  $\phi$  is a non-dimensional factor, its adoption in correlating the stress block parameters will include the effect of column size. The proposal is therefore to use another dimensionless factor, the ratio of effective depth to neutral axis depth ( $d/c$ ), in the correlation to eliminate effects due to column size. The value of  $d/c$  for each specimen is listed in the last column of Tables 4 and 6.

Figures 9(a), 9(b) and 9(c) plot the values of  $k_1$ ,  $k_2$  and  $k_3$  against  $d/c$  respectively. Figures 9(a) and 9(b) indicate that  $k_1$  and  $k_2$  remain fairly constant, at 0.627 and 0.4 respectively. However, Figure 9(c) shows that variation of  $k_3$  with  $d/c$  is fairly linear. A linear regression analysis was carried out to correlate  $k_3$  with  $d/c$ :

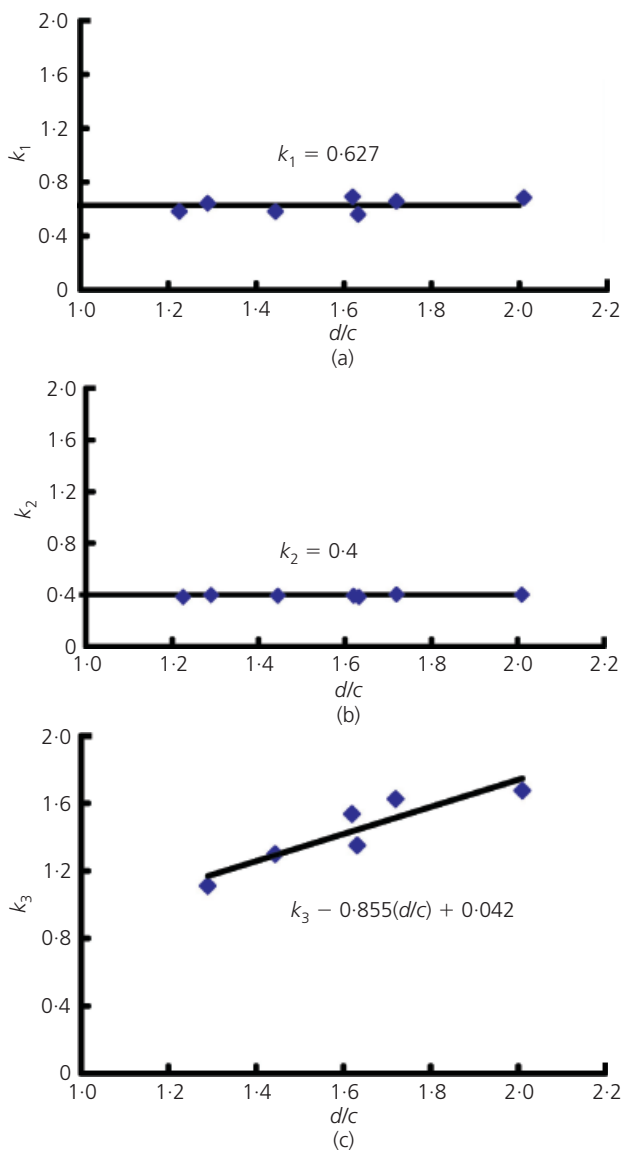


Figure 9. Plots of  $k_1$ ,  $k_2$  and  $k_3$  against  $d/c$

$$8. \quad k_3 = 0.855(d/c) + 0.042$$

The values of  $\alpha$  obtained from the eccentrically loaded specimens are plotted against  $d/c$  in Figure 10(a): the rate of change of  $\alpha$  with respect to  $d/c$  is not constant and dependent on the value of  $d/c$ . Hence, the variation of  $\alpha$  with  $d/c$  cannot be represented precisely by a straight line. For  $d/c \leq 1.3$ ,  $\alpha$  remains relatively constant at 0.85. For  $1.3 < d/c \leq 2.0$ ,  $\alpha$  increases more significantly with  $d/c$  until reaching 1.42, which is the maximum value of  $\alpha$  obtained in this study. Since there are no data available for  $d/c > 2.0$ , it is proposed to set an upper bound limit for  $\alpha$  at 1.42 when  $d/c \geq 2.0$  to ensure a conservative design. In summary, the variation of  $\alpha$  with  $d/c$  can be represented by the following trilinear curve:

$$9a. \quad \alpha = \begin{cases} 0.85 & \text{for } 0 \leq d/c < 1.3 \\ 0.815(d/c) - 0.21 & \text{for } 1.3 \leq d/c < 2.0 \\ 1.42 & \text{for } d/c \geq 2.0 \end{cases}$$

The variation of  $\alpha$  with  $d/c$  given by Equation 9a is plotted in Figure 10(a). Furthermore, since the average value of  $k_2$  is about 0.4 as seen in Figure 9(b), Equation 2 can be rearranged for  $\beta$  as:

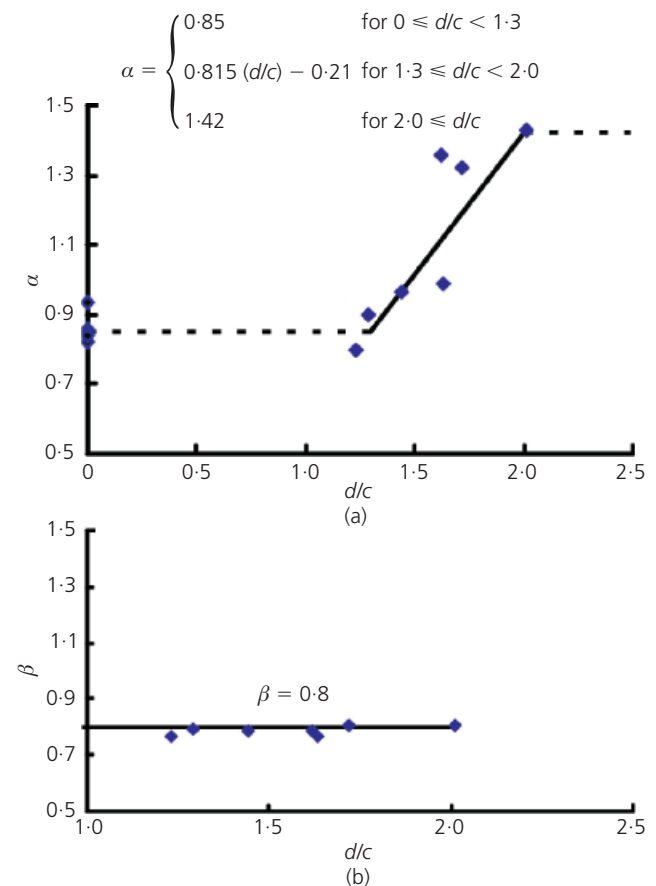


Figure 10. Plots of  $\alpha$  and  $\beta$  against  $d/c$

9b.  $\beta = 2k_2 = 0.80$

which is plotted in Figure 10(b).

Verification against flexural strength of RC beams and columns

To validate the obtained equivalent rectangular concrete stress block parameters, the proposed values of  $\alpha$  and  $\beta$  (given respectively by Equations 9a and 9b) and  $\varepsilon_{cu} = 0.0031$  (the obtained

Specimen code	$f'_c$ : MPa	$M_p$ : kNm (1)	$M_{ACI}$ : kNm (2)	$M_{EC}$ : kNm (3)	$M_{NZ}$ : kNm (4)	$M_t$ : kNm (5)	(1) (5)	(2) (5)	(3) (5)	(4) (5)
Pecce and Fabbrocino (1999)										
A	41.3	105	97.0	97.0	97.0	104.0	1.01	0.93	0.93	0.93
B	41.3	46.3	45.0	45.0	45.0	49.6	0.93	0.91	0.91	0.91
C	42.3	687	637	637	637	713	0.96	0.89	0.89	0.89
Ashour (2000)										
B-N2	48.6	55.4	53.6	53.6	53.6	58.2	0.95	0.92	0.92	0.92
B-N3	48.6	81.1	77.1	77.1	77.1	80.6	1.01	0.96	0.96	0.96
B-N4	48.6	105	98.4	98.4	98.4	99.6	1.06	0.99	0.99	0.99
Ko <i>et al.</i> (2001)										
6-30-1	66.6	17.1	15.7	15.7	15.6	18.4	0.93	0.85	0.85	0.85
6-50-1	66.6	26.3	24.5	24.3	24.4	28.4	0.93	0.86	0.86	0.86
6-65-1	66.6	29.8	27.9	27.6	27.7	32.7	0.91	0.85	0.84	0.85
6-75-1	66.6	34.9	32.6	32.2	32.3	37.8	0.92	0.86	0.85	0.85
Debernardi and Taliano (2002)										
T1	27.7	11.1	10.8	10.8	10.8	13.6	0.82	0.79	0.79	0.79
T2	27.7	21.3	20.5	20.6	20.5	23.6	0.90	0.87	0.87	0.87
T3	27.7	30.9	28.9	29.3	28.9	32.5	0.95	0.89	0.90	0.89
T4	27.7	48.6	46.9	46.8	46.9	59.8	0.81	0.78	0.78	0.78
T5	27.7	96.1	93.1	93.1	93.1	108	0.89	0.87	0.87	0.87
T6	27.7	181	171	171	171	192	0.94	0.89	0.89	0.89
T7	27.7	233	217	222	217	222	1.05	0.98	1.00	0.98
T8	27.7	84.5	81.1	81.2	81.1	93.9	0.90	0.86	0.86	0.86
T9	27.7	157	152	152	152	183	0.86	0.83	0.83	0.83
T10	27.7	335	325	325	325	330	1.01	0.98	0.98	0.98
Shin <i>et al.</i> (2007)										
RC01	31.2	427	420	420	420	480	0.89	0.88	0.88	0.88
Lam <i>et al.</i> (2008)										
L-C1	29.8	14.8	14.6	14.6	14.6	14.2	1.04	1.03	1.03	1.03
L-D	29.8	9.9	9.8	9.8	9.8	11.6	0.85	0.84	0.84	0.84
L-E	29.8	26.7	25.9	26.0	25.9	29.4	0.91	0.88	0.89	0.88
Fathifazl <i>et al.</i> (2009)										
EV-1.5N	43.5	83.4	79.4	79.5	79.4	86.9	0.96	0.91	0.91	0.91
EV-2.7N	43.5	113	108	108	108	126	0.90	0.86	0.86	0.86
CG-2.9N	43.5	112	106	106	106	119	0.94	0.90	0.90	0.90
Lee <i>et al.</i> (2009)										
C15A	29.0	50.2	47.1	47.2	47.1	55.6	0.90	0.85	0.85	0.85
Shin and Lee (2010)										
RC-C	23.5	574	555	558	555	608	0.94	0.91	0.92	0.91
RC-C-S1	23.5	784	747	753	747	755	1.04	0.99	1.00	0.99
RC-C-S2	23.5	941	881	887	880	925	1.02	0.95	0.96	0.95
Average							0.94	0.90	0.90	0.90

Table 7. Comparison of proposed strengths of beams

average value of  $\epsilon_{cu}$ ) are used to evaluate the flexural strengths of RC members tested by other researchers. These RC members include:

- (a) beams (Ashour, 2000; Debernardi and Taliano, 2002; Fathifazl *et al.*, 2009; Ko *et al.*, 2001; Lam *et al.*, 2008; Lee *et al.*, 2009; Pecce and Fabbrocino, 1999; Shin and Lee, 2010; Shin *et al.*, 2007)
- (b) columns subjected to low axial load level ( $0 < P/A_g f'_c \leq 0.2$ ;  $A_g$  is the column cross-section area) (Ho and Pam, 2003a; Marefat *et al.*, 2005; Mo and Wang, 2000; Tao and Yu, 2008; Watson and Park, 1994; Woods *et al.*, 2007)
- (c) columns subjected to medium axial load level ( $0.2 < P/A_g f'_c \leq 0.5$ ) (Lam *et al.*, 2003; Marefat *et al.*, 2005, 2006; Mo and Wang, 2000; Sheikh and Khoury, 1993; Tao and Yu, 2008; Watson and Park, 1994)
- (d) columns subjected to high axial load level ( $0.5 < P/A_g f'_c \leq 0.7$ ) (Ho and Pam, 2003b; Lam *et al.*, 2003; Sheikh and Yeh, 1990; Sheikh *et al.*, 1994)

- (e) columns subjected to ultra-high axial load level ( $0.7 < P/A_g f'_c$ ) (Nemecek *et al.*, 2005; Sheikh and Khoury, 1993; Sheikh and Yeh, 1990; Sheikh *et al.*, 1994; Tao and Yu, 2008).

These predicted flexural strengths  $M_p$  were compared with their respective measured strengths  $M_t$  and respective theoretical strengths based on various RC design codes –  $M_{ACI}$  based on AIC 318M-08 (ACI, 2008),  $M_{EC}$  based on Eurocode 2 (CEN, 2004) and  $M_{NZ}$  based on NZS 3101 (SNZ, 2006). The comparison is summarised in Table 7 for beams and Tables 8–11 for columns.

Analysis of Tables 7–11 leads to the following conclusions.

- (a) The flexural strengths of RC beams and columns subjected to low and medium axial load levels predicted by the proposed values of  $\alpha$ ,  $\beta$  and  $\epsilon_{cu}$  have the best agreement with their measured flexural strengths.

Specimen code	$f'_c$ : MPa	$\frac{P}{A_g f'_c}$	$M_p$ : kNm (1)	$M_{ACI}$ : kNm (2)	$M_{EC}$ : kNm (3)	$M_{NZ}$ : kNm (4)	$M_t$ : kNm (5)	(1) (5)	(2) (5)	(3) (5)	(4) (5)
Watson and Park (1994)											
1	47.0	0.100	321	302	307	302	335	0.96	0.90	0.92	0.90
Mo and Wang (2000)											
C1-1	24.9	0.113	328	301	305	301	351	0.93	0.86	0.87	0.86
C1-2	26.7	0.106	332	304	308	304	375	0.89	0.81	0.82	0.81
C1-3	26.1	0.108	331	303	307	303	428	0.77	0.71	0.72	0.71
C2-1	25.3	0.167	353	319	327	319	347	1.02	0.92	0.94	0.92
C2-2	27.1	0.156	358	325	331	325	400	0.89	0.81	0.83	0.81
C2-3	26.8	0.158	357	324	330	324	427	0.83	0.76	0.77	0.76
Ho and Pam (2003a)											
BS-80-01-09-S1	72.6	0.169	250	225	221	219	257	0.98	0.88	0.86	0.85
BS-80-01-09-S2	74.6	0.159	241	219	215	213	237	1.02	0.92	0.91	0.90
BS-80-01-09-S3	72.4	0.160	241	217	214	212	238	1.01	0.91	0.90	0.89
Marefat <i>et al.</i> (2005)											
STMC-9	24.0	0.190	25.5	22.8	22.5	22.5	23.3	1.09	0.97	0.98	0.97
SBCC-7	27.0	0.160	45.5	41.6	41.9	41.7	45.1	1.01	0.92	0.93	0.92
Woods <i>et al.</i> (2007)											
S3-2-76	69.0	0.156	74.1	65.4	65.7	64.1	95.6	0.77	0.68	0.69	0.67
S4-8-76	69.0	0.156	73.6	66.7	66.8	65.4	91.0	0.81	0.73	0.73	0.72
S6-4-76	69.0	0.156	73.2	66.0	66.3	64.7	90.6	0.81	0.73	0.73	0.71
S8-0-76	69.0	0.156	72.7	65.4	65.7	64.1	88.3	0.82	0.74	0.74	0.73
V5-5-66	69.0	0.156	73.4	66.4	66.6	65.1	91.5	0.80	0.73	0.73	0.71
Tao and Yu (2008)											
US-3U	49.2	0.108	17.8	16.5	16.5	16.5	15.9	1.12	1.04	1.04	1.04
BS-3U	49.8	0.098	16.6	15.4	15.4	15.4	14.6	1.14	1.05	1.05	1.05
BS-4U	49.8	0.067	14.8	13.6	13.7	13.6	13.3	1.11	1.02	1.03	1.02
Average								0.94	0.85	0.86	0.85

Table 8. Comparison of proposed strengths of columns subjected to low axial load level

Specimen code	$f'_c$ : MPa	$\frac{P}{A_g f'_c}$	$M_p$ : kNm (1)	$M_{ACI}$ : kNm (2)	$M_{EC}$ : kNm (3)	$M_{NZ}$ : kNm (4)	$M_t$ : kNm (5)	$\frac{(1)}{(5)}$	$\frac{(2)}{(5)}$	$\frac{(3)}{(5)}$	$\frac{(4)}{(5)}$
Sheikh and Khoury (1993)											
AS-19	32.3	0.470	231	179	184	179	220	1.05	0.81	0.84	0.82
Watson and Park (1994)											
2	44.0	0.300	490	406	410	406	486	1.01	0.84	0.84	0.84
3	44.0	0.300	490	406	410	406	479	1.02	0.85	0.86	0.85
4	40.0	0.300	459	382	385	382	448	1.02	0.85	0.86	0.85
5	41.0	0.500	560	373	383	373	526	1.07	0.71	0.73	0.71
6	40.0	0.500	551	367	377	368	526	1.05	0.70	0.72	0.70
Mo and Wang (2000)											
C3-1	26.4	0.213	373	333	344	333	353	1.06	0.94	0.97	0.94
C3-2	27.5	0.205	382	338	348	338	396	0.97	0.85	0.88	0.85
C3-3	26.9	0.209	381	335	346	335	424	0.90	0.79	0.82	0.79
Lam <i>et al.</i> (2003)											
X6	31.9	0.450	36.6	28.5	29.0	28.6	37.1	0.99	0.77	0.78	0.77
X7	35.7	0.450	39.0	29.7	30.5	29.8	37.1	1.05	0.80	0.82	0.80
Marefat <i>et al.</i> (2005)											
NTCM-14	20.1	0.310	18.6	16.0	16.0	16.0	16.8	1.11	0.95	0.95	0.95
NBCC-12	25.2	0.230	25.4	22.0	22.4	22.0	21.7	1.17	1.01	1.03	1.01
NBCM-11	24.5	0.250	45.1	38.6	38.5	38.6	44.6	1.01	0.87	0.86	0.87
SBCM-8	28.0	0.220	52.0	46.0	46.0	46.0	58.7	0.89	0.78	0.78	0.78
Marefat <i>et al.</i> (2006)											
NTMM-13	21.0	0.310	19.0	16.3	16.4	16.3	17.3	1.10	0.94	0.95	0.94
Tao and Yu (2008)											
US-2U	49.2	0.224	24.1	21.9	22.1	21.9	21.1	1.14	1.04	1.05	1.04
BS-2U	49.8	0.230	24.0	21.7	21.8	21.7	25.1	0.96	0.86	0.87	0.86
Average								1.03	0.85	0.87	0.85

**Table 9.** Comparison of proposed strengths of columns subjected to medium axial load level

- (b) For RC beams, the average ratio of predicted ( $M_p$ ) to measured ( $M_t$ ) flexural strength is 0.94, whereas the ratios of the theoretical strength based on current RC design codes ( $M_{ACI}$ ,  $M_{EC}$ ,  $M_{NZ}$ ) to measured flexural strength are all equal to 0.90. It is evident that the proposed method can increase the accuracy of flexural strength prediction by 4% on average.
- (c) For RC columns subjected to low and medium axial load level, the average ratio of the predicted to measured flexural strength is 0.94 and 1.03, respectively, whereas the ratios of the theoretical strength based on current RC design codes to measured flexural strength are all about 0.85 for low and medium axial load levels. It is evident that the proposed method can increase the accuracy of flexural strength prediction by respectively 9% and 14% on average.
- (d) For RC columns subjected to high and ultra-high axial load levels, the average ratio of the predicted to measured flexural strength is 0.87 and 0.98, respectively, whereas the ratios of the theoretical strength based on current RC design codes ( $M_{ACI}$ ,  $M_{EC}$ ,  $M_{NZ}$ ) to measured flexural strength are about 0.86 and 0.98 respectively. The flexural strength predicted by

the proposed method is very close to that predicted by current RC design codes.

- (e) The accuracy of flexural strength predictions using the proposed values of  $\alpha$ ,  $\beta$  and  $\epsilon_{cu}$  is improved for RC beams and columns subjected to low and medium axial load levels. This indicates that the proposed equivalent rectangular concrete stress block parameters  $\alpha$  and  $\beta$ , which depend on strain gradient, represent the equivalent concrete stress developed under flexure more precisely.
- (f) The accuracy of flexural strength prediction does not improve very much for RC columns subjected to high and ultra-high axial load levels. This is because the strain gradient is very small in these columns, and the proposed values of  $\alpha$  and  $\beta$  resemble the respective values currently adopted in various RC design codes.

## Conclusions

The effects of strain gradient on the maximum concrete stress and equivalent concrete stress that can be developed in RC members under flexure were studied experimentally. Five groups

Specimen code	$f'_c$ : MPa	$\frac{P}{A_g f'_c}$	$M_p$ : kNm (1)	$M_{ACI}$ : kNm (2)	$M_{EC}$ : kNm (3)	$M_{NZ}$ : kNm (4)	$M_t$ : kNm (5)	$\frac{(1)}{(5)}$	$\frac{(2)}{(5)}$	$\frac{(3)}{(5)}$	$\frac{(4)}{(5)}$
Sheikh and Yeh (1990)											
E-2	31.4	0.610	162	160	164	161	169	0.95	0.95	0.97	0.95
A-3	31.8	0.610	164	163	162	163	198	0.83	0.82	0.82	0.82
F-4	32.2	0.600	166	165	168	165	198	0.84	0.83	0.85	0.83
F-12	33.4	0.600	156	156	158	157	161	0.97	0.97	0.98	0.97
A-16	33.9	0.600	157	157	159	158	158	1.00	1.00	1.01	1.00
Sheikh <i>et al.</i> (1994)											
AS-3	33.2	0.600	167	167	169	168	193	0.87	0.87	0.88	0.87
AS-3H	54.1	0.620	215	209	210	208	237	0.91	0.88	0.89	0.88
A-17H	59.1	0.650	219	213	204	207	261	0.84	0.82	0.78	0.79
Ho and Pam (2003b)											
BS-60-06-61-S	51.1	0.675	394	373	401	373	418	0.94	0.89	0.96	0.89
BS-60-0661-C	53.2	0.647	400	385	406	376	427	0.94	0.90	0.95	0.88
Lam <i>et al.</i> (2003)											
X4	31.9	0.650	24.3	24.3	24.6	24.3	34.5	0.71	0.71	0.71	0.72
X5	31.9	0.650	24.3	24.3	24.6	24.3	36.3	0.67	0.67	0.68	0.69
Average								0.87	0.86	0.87	0.86

**Table 10.** Comparison of proposed strengths of columns subjected to high axial load level

Specimen code	$f'_c$ : MPa	$\frac{P}{A_g f'_c}$	$M_p$ : kNm (1)	$M_{ACI}$ : kNm (2)	$M_{EC}$ : kNm (3)	$M_{NZ}$ : kNm (4)	$M_t$ : kNm (5)	$\frac{(1)}{(5)}$	$\frac{(2)}{(5)}$	$\frac{(3)}{(5)}$	$\frac{(4)}{(5)}$
Sheikh and Yeh (1990)											
F-6	27.2	0.750	133	134	135	134	145	0.92	0.92	0.93	0.92
D-7	26.2	0.780	121	121	123	121	133	0.91	0.91	0.92	0.91
E-8	25.9	0.780	128	128	129	128	129	0.99	0.99	1.00	0.99
F-9	26.5	0.770	130	131	132	131	152	0.86	0.86	0.87	0.86
E-10	26.3	0.770	130	131	131	131	133	0.98	0.98	0.99	0.98
A-11	27.9	0.740	138	139	140	139	135	1.02	1.03	1.03	1.03
E-13	27.2	0.740	135	135	136	135	128	1.05	1.05	1.06	1.05
D-14	26.9	0.750	126	127	129	127	117	1.08	1.09	1.11	1.09
D-15	26.2	0.75	124	125	125	124	135	0.92	0.93	0.93	0.92
Sheikh and Khoury (1993)											
ES-13	32.5	0.760	140	140	141	140	163	0.86	0.86	0.86	0.86
FS-9	32.4	0.760	140	140	141	140	157	0.89	0.89	0.90	0.89
Sheikh <i>et al.</i> (1994)											
AS-17	31.3	0.770	136	136	137	136.4	180	0.76	0.76	0.76	0.76
Nemecek <i>et al.</i> (2005)											
N50	30.0	0.915	9.9	9.4	10.9	9.4	9.6	1.03	0.98	1.14	0.98
N100	30.0	0.900	10.3	9.9	11.4	9.9	9.3	1.11	1.06	1.23	1.06
N150	30.0	0.892	10.5	10.1	11.6	10.1	9.3	1.13	1.09	1.25	1.09
Tao and Yu (2008)											
BS-1U	49.8	0.806	12.4	12.4	12.4	12.4	13.7	0.91	0.91	0.91	0.91
Average								0.98	0.97	1.01	0.97

**Table 11.** Comparison of proposed strengths of columns subjected to ultra-high axial load level



(12 specimens) of inverted T-shaped specimens were fabricated; one group was plain concrete and the rest were reinforced. The specimens in each group had the same cross-section properties. One specimen in each group was subjected to concentric axial load while the rest were subjected to eccentric axial load.

The effects of strain gradient on the maximum concrete stress that can be developed under flexure were investigated through the parameter  $k_3$ , which is the ratio of the maximum concrete stress developed under flexure to uniaxial concrete strength. The value of  $k_3$  for each eccentrically loaded specimen was determined by equating the theoretical with the measured values of axial force and moment. The effects of strain gradient on equivalent concrete stress developed under flexure were investigated by the parameter  $\alpha$ , which is the ratio of the equivalent concrete stress to the uniaxial concrete cylinder strength.

The obtained values of  $k_3$  and  $\alpha$  for the eccentrically loaded specimens were all larger than those reported by previous researchers. Also, the values of  $\alpha$  were significantly larger than the respective value stipulated in the current RC design codes (i.e.  $\alpha = 0.85$ ). More importantly, it was found that the values of  $k_3$  and  $\alpha$  were dependent on the strain gradient as well as concrete strength.

An empirical formula was proposed for the relation between  $\alpha$  and strain gradient, with the latter represented by a dimensionless factor  $d/c$  (i.e. the ratio of effective depth to neutral axis depth) to eliminate size effects. A tri-linear curve was proposed for the variation of  $\alpha$  with  $d/c$  for design purposes. The values of  $k_1$ ,  $k_2$ ,  $\beta$  and  $\varepsilon_{cu}$  remained relatively constant at about 0.63, 0.40, 0.80 and 0.0031, respectively.

The validity of the proposed values of  $\alpha$ ,  $\beta$  and  $\varepsilon_{cu}$ , which take into account the effects of strain gradient, in flexural strength evaluation of RC members was checked by comparing the theoretical strengths of beams and columns subjected to low, medium, high and ultra-high axial load levels with the strengths measured by previous researchers. The predicted flexural strengths were also compared with those estimated by various RC design codes (AIC 318M-08, Eurocode 2 and NZS 3101) by means of ratios with their measured strengths. The comparisons indicated that the proposed values of  $\alpha$ ,  $\beta$  and  $\varepsilon_{cu}$  predict the flexural strength of RC beams and columns subjected to low and medium axial load levels more accurately than the current RC design codes. The accuracy improvement was about 4% for RC beams, but could reach about 18% for columns subjected to medium axial load levels. For columns subjected to high and ultra-high axial load levels, the flexural strength prediction is similar to that predicted by the current RC design codes due to small strain gradient.

### Acknowledgements

A research grant from the Seed Funding Programme for Basic Research (account code 10208226) of The University of Hong

Kong (HKU) for the work presented here is gratefully acknowledged. The authors gratefully thank the Department of Civil and Structural Engineering of The Hong Kong Polytechnic University (PolyU), where most of the experimental tests were conducted. Support from technical staff in the structural laboratory of PolyU and HKU Department of Civil Engineering are greatly appreciated.

### REFERENCES

- ACI (American Concrete Institute) (2008) ACI 318M-08: Building code requirements for reinforced concrete and commentary. ACI, Farmington Hills, MI.
- Ashour SA (2000) Effect of compressive strength and tensile reinforcement ratio on flexural behaviour of high-strength concrete beams. *Engineering Structures* **25**(8): 1083–1096.
- Attard MM and Stewart MG (1998) A two parameter stress block for high-strength concrete. *ACI Structural Journal* **95**(3): 305–317.
- Baczkowski BJ and Kuang JS (2008) A new approach to testing concrete coupling beams subjected to reversed cyclic loading. *Magazine of Concrete Research* **60**(4): 301–309.
- Bae S and Bayrak O (2003) Stress block parameters for high-strength concrete members. *ACI Structural Journal* **100**(5): 626–636.
- Bai ZZ and Au FTK (2008) Ductility of symmetrically reinforced concrete columns. *Magazine of Concrete Research* **61**(5): 345–357.
- Bukhari IA, Vollum RL, Ahmad S and Sagaseta J (2010) Shear strengthening of reinforced concrete beams with CFRP. *Magazine of Concrete Research* **62**(1): 65–77.
- Choi E, Park J, Nam TH and Yoon SJ (2009) A new steel jacketing method for RC columns. *Magazine of Concrete Research* **61**(10): 787–796.
- Choi HB, Yi CK, Cho HH and Kang KI (2010) Experimental study on the shear strength of recycled aggregate concrete beams. *Magazine of Concrete Research* **62**(2): 103–114.
- Debernardi PG and Taliano M (2002) On evaluation of rotation capacity for reinforced concrete beams. *ACI Structural Journal* **99**(3): 360–368.
- CEN (European Committee for Standardization) (2004) Eurocode 2: *Design of concrete structures: Part 1–1: General rules and rules for buildings*. CEN, Brussels.
- Fathifazl G, Razaqpur AG, Isgor OB et al. (2009) Shear strength of reinforced recycled concrete beams without stirrups. *Magazine of Concrete Research* **61**(7): 477–490.
- Han TH, Stallings JM, Cho SK and Kang YJ (2010) Behaviour of a hollow RC column with an internal tube. *Magazine of Concrete Research* **62**(1): 25–38.
- Ho JCM and Pam HJ (2003a) Inelastic design of low-axially loaded high-strength reinforced concrete columns. *Engineering Structures* **25**(8): 1083–1096.
- Ho JCM and Pam HJ (2003b) Influence of transverse steel configuration on post-elastic behaviour of high-strength reinforced concrete columns. *Transactions of the Hong Kong Institution of Engineers* **10**(2): 1–9.
- Ho JCM and Pam HJ (2010) Deformability evaluation of high-

- strength reinforced concrete columns. *Magazine of Concrete Research* **62(8)**: 569–583.
- Hognestad E, Hanson NW and McHenry D (1955) Concrete stress distribution in ultimate strength design. *ACI Journal* **52(4)**: 455–479.
- Ibrahim HHH and MacGregor JG (1996) Flexural behavior of laterally reinforced high-strength concrete sections *ACI Structural Journal* **93(6)**: 674–684.
- Ibrahim HHH and MacGregor JG (1997) Modification of the ACI rectangular stress block for high-strength concrete. *ACI Structural Journal* **94(1)**: 40–48.
- Jaafar K (2008) Shear behaviour of reinforced concrete beams with confinement near plastic hinges. *Magazine of Concrete Research* **60(9)**: 665–672.
- Kaar PH, Hanson NW and Capell HT (1978) Stress–strain characteristics of high strength concrete. *Douglas McHenry International Symposium on Concrete and Concrete Structures*. ACI, Detroit, pp. 161–185.
- Ko MY, Kim SW and Kim JK (2001) Experimental study on the plastic rotation capacity of reinforced high strength concrete beams. *Materials and Structures* **34(5)**: 302–311.
- Lam SSE, Wu B, Wong YL et al. (2003) Drift capacity of rectangular reinforced concrete columns with low lateral confinement and high-axial load. *ASCE Journal of Structural Engineering* **129(6)**: 733–742.
- Lam SSE, Wu B, Liu ZQ and Wong YL (2008) Experimental study on seismic performance of coupling beams not designed for ductility. *Structural Engineering and Mechanics* **28(3)**: 317–333.
- Lee C, Jeong SM and Park JW (2009) Use of fibre sheet strip stirrups for internal shear reinforcement of concrete beams. *Magazine of Concrete Research* **61(9)**: 731–743.
- Lu WY, Lin IJ and Hwang SJ (2009) Shear strength of reinforced concrete corbels. *Magazine of Concrete Research* **61(10)**: 807–813.
- Mansur MA, Chin MS and Wee TH (1997) Flexural behavior of high-strength concrete beams. *ACI Structural Journal* **94(6)**: 663–673.
- Marefat MS, Khanmohammadi M, Bahrani MK and Goli A (2005) Cyclic load testing and numerical modelling of concrete columns with substandard seismic details. *Computers and Concrete* **2(5)**: 367–380.
- Marefat MS, Khanmohammadi M, Bahrani MK and Goli A (2006) Experimental assessment of reinforced concrete columns with deficient seismic details under cyclic load. *Advances in Structural Engineering* **9(3)**: 337–347.
- Mo YL and Wang SJ (2000) Seismic behavior of RC columns with various tie configurations. *ASCE Journal of Structural Engineering* **126(10)**: 1122–1130.
- Nemecek P, Padevet B, Patzak B and Bittnar Z (2005) Effect of transversal reinforcement in normal and high strength concrete columns. *Materials and Structures* **38(7)**: 665–671.
- Ozbakkaloglu T and Saatcioglu M (2004) Rectangular stress block for high-strength concrete. *ACI Structural Journal* **101(4)**: 475–483.
- Pam HJ and Ho JCM (2001) Flexural strength enhancement of confined reinforced concrete columns. *Proceedings of the Institution of Civil Engineers, Structures and Buildings* **146(4)**: 363–370.
- Pam HJ and Ho JCM (2009) Length of critical region for confinement steel in limited ductility high-strength reinforced concrete columns. *Engineering Structures* **31(12)**: 2896–2908.
- Park R and Paulay T (1975) *Reinforced Concrete Structures*. Wiley, New York.
- Pecce M and Fabbrocino G (1999) Plastic rotation capacity of beams in normal and high-performance concrete. *ACI Structural Journal* **96(2)**: 290–296.
- Sebastian W and Zhang C (2008) Analysis of concrete structures across the ductility spectrum. *Magazine of Concrete Research* **60(9)**: 685–690.
- Sheikh SA and Khoury SS (1993) Confined concrete columns with stubs. *ACI Structural Journal* **90(4)**: 414–431.
- Sheikh SA and Uzumeri SM (1980) Strength and ductility of tied concrete columns. *Journal of Structural Engineering Division ASCE* **106(5)**: 1079–1101.
- Sheikh SA and Yeh CC (1990) Tied concrete columns under axial load and flexure. *ASCE Journal of Structural Engineering* **116(10)**: 2780–2801.
- Sheikh SA, Shah DV and Khoury SS (1994) Confinement of high-strength concrete columns. *ACI Structural Journal* **91(1)**: 100–111.
- Shin KJ and Lee SH (2010) Flexural behaviour of RC beams strengthened with high-tension steel rod. *Magazine of Concrete Research* **62(2)**: 137–147.
- Shin KJ, Lim JH, Oh YS and Moon JH (2007) An experimental study on the flexural behaviour of RC beams strength with high-strength bars. *Magazine of Concrete Research* **59(7)**: 469–481.
- Sim JI, Yang KH and Shim HJ (2009) Test on seismic strengthening of RC columns using wire rope and T-plate units. *Magazine of Concrete Research* **61(10)**: 823–836.
- Soliman MTM and Yu CW (1967) The flexural stress–strain relationship of concrete confined by rectangular transverse reinforcement. *Magazine of Concrete Research* **19(61)**: 223–238.
- Spence R (2008) Earthquake loss estimation for reinforced concrete buildings: some problems. *Magazine of Concrete Research* **60(9)**: 701–707.
- SNZ (Standards New Zealand) (2006) NZS 3101: Concrete structures standard: Part 1: The design of concrete structures. SNZ, Wellington.
- Swartz SE, Nikaean A, Narayan BHD, Periyakaruppan N and Refai TME (1985) Structural bending properties of high strength concrete. *ACI Special Publication* **87(9)**: 147–178.
- Tan TH and Nguyen NB (2004) Determination of stress–strain curves of concrete from flexure tests. *Magazine of Concrete Research* **56(4)**: 243–250.
- Tan TH and Nguyen NB (2005) Flexural behavior of confined

high-strength concrete columns. *ACI Structural Journal* **102(2)**: 198–205.

Tao Z and Yu Q (2008) Behaviour of CFRP-strengthened slender square RC columns. *Magazine of Concrete Research* **60(7)**: 523–533.

Watson S and Park R (1994) Simulated seismic load tests on reinforced concrete columns. *ASCE Journal of Structural Engineering* **120(6)**: 1825–1849.

Woods JM, Kioussis PD, Ehsani MR and Saadatmanesh H (2007)

Bending ductility of rectangular high strength concrete columns. *Engineering Structures* **29(8)**: 1783–1790.

Wu YF, Oehlers DJ and Griffith MC (2004) Rational definition of the flexural deformation capacity of RC column sections. *Engineering Structures* **26(5)**: 641–650.

Zhou W and Zheng WZ (2010) Experimental research on plastic design method and moment redistribution in continuous concrete beams prestressed with unbonded tendons. *Magazine of Concrete Research* **62(1)**: 51–64.

---

**WHAT DO YOU THINK?**

To discuss this paper, please submit up to 500 words to the editor at [www.editorialmanager.com/macr](http://www.editorialmanager.com/macr) by 1 July 2012. Your contribution will be forwarded to the author(s) for a reply and, if considered appropriate by the editorial panel, will be published as a discussion in a future issue of the journal.